Anal. Chem. **2000,** *72,* 3995−4002

Electrochemical Study of Chemically Modified and Screen-Printed Graphite Electrodes with $[Sb^{V}O(CHL)_2]$Hex. Application for the Selective Determination of Sulfide

Mamas I. Prodromidis, Panayiotis G. Veltsistas, and Miltiades I. Karayannis*

Department of Chemistry, University of Ioannina, Ioannina 45110, Greece

The preparation and electrochemical characterization of graphite electrodes modified with hexadecylpyridinium−bis(chloranilato)−antimonyl(V), $[Sb^{V}O(CHL)_2]$Hex, (CMEs) as well as their behavior as electrocatalysts toward the oxidation of sulfide are described. The self-exchange rate constant k^o of immobilized $[Sb^{V}O(CHL)_2]$Hex and the effect of the surface coverage were evaluated. $[Sb^{V}O(CHL)_2]$Hex is a new compound. Synthesis protocol and some identification studies are given. The fabrication of screen-printed electrodes (SPEs) with a mixture of 5% (w/w) $[Sb^{V}O(CHL)_2]$Hex/graphite powder in 1.5% (w/v) ethyl cellulose in 2-butoxyethyl acetate is also described. SPEs, poised at +0.08 mV versus Ag/AgCl, at pH 6.5 were utilized for the determination of sulfide in simulated wastewater samples. Interference of various compounds was also tested. The proposed method correlates well with a colorimetric method. Calibration graphs were linear over the range 0.01−0.7 mM sodium sulfide and the CV was 2.8% (n = 8) for 0.1 mM sodium sulfide. Recovery ranged from 94 to 102%. Both $[Sb^{V}O(CHL)_2]$Hex CMEs and SPE showed very good storage stability. $[Sb^{V}O(CHL)_2]$Hex CMEs showed poor working stability in contrast to printed electrodes, which operated with no remarkable loss of their initial activity for more than 100 runs.

Sulfide is formed in wastewater by the action of anaerobic bacteria on organic matter. Sulfide salts are used in industrial waste streams in order to control the levels of several toxic metals (e.g., mercury, lead) discharged into the environment, since many metal sulfides are insoluble and precipitate out in the waste stream.[1] There are limits on the total level of sulfide permitted in waste discharges because of its toxicity, capacity to remove dissolved oxygen, and capability to produce hydrogen sulfide. Numerous problems are associated with the corrosiveness of sulfide and hydrogen sulfide. Obviously the level of sulfide in industrial and urban waste has a tremendous impact on public acceptance and safety as well as on the longevity of concrete infrastructure.[2,3]

A number of standard methods are available for the determination of sulfide. Most popular and well-known is the colorimetric method with methylene blue.[4] Other methods such as spectrophotometry,[5] fluorometry,[6] potentiometry,[7] molecular absorption spectroscopy,[8] chemiluminescence,[9] liquid chromatography,[10] and coulometry[11] have been reported.

Amperometric methods for the determination of volatile hydrogen sulfide based on mediated oxidation through ferricyanide[12] or the use of cobalt phthalocyanide as a catalyst on screen-printed electrodes[13] or macrobicyclic polyaza−cobalt (III) complexes[14] have also been published. These methods are either difficult to automate[5−9,11] or suffer from numerous chemical interferences.[11−14] Some are highly prevented by solution turbidity[5−9] or demand sophisticated instrumentation.[10]

The present work explores the synthetic applicability of a novel complex, the electrochemical behavior of hexadecylpyridinium−bis(chloranilato)−antimonyl(V) ($[Sb^{V}O(CHL)_2]$Hex) chemically modified electrodes (CMEs) and the fabrication of screen-printed electrodes modified with $[Sb^{V}O(CHL)_2]$Hex, a highly selective and reactive mediator, for the oxidation of sulfide. The latter approach provides the feasibility for an economical, interference-free, easy to perform, and fast method for the determination of sulfide in urban waste. The proposed method is based on the redox reaction between sulfide and $[Sb^{V}O(CHL)_2]$Hex in connection with the

* Corresponding author: (tel) xx30-651-98406; (fax) xx30-651-98407; (e-mail) mkaragia@cc.uoi.gr.

(1) Kirk, R. E.; Othmer, D. F. *Encyclopedia of Chemical Technology*, 3rd ed.; Wiley: New York, 1981; Vol. 17.
(2) *Process Design Manual for Sulphide Control in Sanitary Sewerage System*; Environmental Protection Agency: Washington, DC, 1974.
(3) Roy, A. B.; Trudinger, P. A. *The Biochemistry of Inorganic Compounds of Sulphur*; Cambridge University Press: London, 1970.
(4) *Stantard Methods for the Examination of Water and* Waste Water, 17th ed.; Clesceri, L. S., Greenberg, A. E., Trussell, R. R., Eds.; American Public Health Association: Washington, DC, 1989; pp 4−191.
(5) Ensafi, A. A. *Anal. Lett.* **1992**, *25*, 1525−1543.
(6) Dasgupta, P. K.; Chin Yang, H. *Anal. Chem.* **1986**, *58*, 2839−2844.
(7) Glaister, M. G.; Moody, J. G.; Thomas, J. D. R. *Analyst (Cambridge, U.K.)* **1995**, *110*, 113−119.
(8) Ebdon, L.; Hill, S. J.; Jameel, M.; Corns, W. T.; Stockwell, P. B. *Analyst (Cambridge, U.K.)* **1997**, *122*, 689−693.
(9) Xue-Xin, Q.; Yue-Ying, G.; Yamada, M.; Kobayashi, E.; Suzuki, S. *Talanta* **1989**, *36*, 505−508.
(10) Gru, C.; Sarradin, P. M.; Legoff, H.; Narcon, S.; Caprais, J.-C.; Lallier, F. H. *Analyst (Cambridge, U.K.)* **1998**, *123*, 1289−1293.
(11) Pierce, D. T.; Applebee, M. S.; Lacher, C.; Bessie, J. *Environ. Sci. Technol.* **1998**, *32*, 1734−1737.
(12) Jeroschewski, P.; Haase, K.; Trommer, A.; Grundler, P. *Electroanalysis* **1994**, *6*, 769−772.
(13) Hart, J. P.; Abass, A. K. *Anal. Chim. Acta* **1997**, *342*, 199−206.
(14) Kroll, A. V.; Smorchkov, V. I.; Nazarenko, A. Y. *Sens. Actuators* **1994**, *21*, 97−100.

10.1021/ac0001784 CCC: $19.00 © 2000 American Chemical Society
Published on Web 08/02/2000

electrochemical oxidation of $[Sb^{III}(CHL)_2]$Hex on the electrode surface at +0.08 V versus Ag/AgCl, according to the following reaction scheme:

$$3[Sb^{V}O(CHL)_2]\text{Hex} + [S^{2-}] \xrightarrow{\text{electrode at } +0.08\text{ V } (-2e^-)} 3\,[Sb^{III}(CHL)_2]\text{Hex} + [SO_3^{2-}] \quad (1)$$

EXPERIMENTAL SECTION

Reagents. $[Sb^{V}O(CHL)_2]$Hex was synthesized in our laboratory (see below). Sodium sulfide and ethyl cellulose were purchased from Sigma (St. Louis, MO). Diethylene glycol monoethyl ether acetate (DGMEA) and 2-butoxyethyl acetate (2-BEA) were purchased from Fluka (Deisenhofen, Germany) and Aldrich (Gollingham, Germany), respectively. Graphite powder, chloranilic acid, and potassium pyroantimonate were supplied by Fluka. All other chemicals were of analytical grade from Merck (Darmstandt, Germany) and Aldrich.

Silver (PF410), graphite (421SS), and silver/silver chloride (6038SS) inks were purchased from Acheson Colloiden B.V (Scheemda, The Netherlands). A nail hardener (Revlon, New York, NY) was used as an insulating ink. PVC matrix (Genotherm EZ-53, Matt clear resist, 0.4-mm thickness) was obtained from Sericol Ltd. (London, U.K.). Screens were constructed by DEK Printing Machines Ltd. (Dorset, U.K.), with 250 mesh/in. stainless steel for the silver and graphite inks and a 220 mesh/in. polyester for silver/silver chloride ink. A 75 durometer squeegee (DEK) was used. The emulsion thickness was 20−40 μm.

The stock sulfide solution (~340 mM) was prepared by dissolving $Na_2S{\cdot}9H_2O$ crystals in degassed, distilled water and kept at +4 °C; the solution was stable for a maximum of two weeks. This solution was periodically standardized with the methylene blue colorimetric method. Working standard solutions were prepared before use in degassed, distilled water.

Apparatus. Screen-printed electrodes were fabricated using a model 247 screen printer (DEK). All electrochemical experiments were conducted with a computer-controlled potentiostat, the Autolab electrochemical analyzer (ECO Chemie, Utrecht, The Netherlands). Cyclic voltammetry and amperometric experiments were performed with a voltammetry cell (VC2, BAS) using a graphite electrode (RW0001, 6.5-mm diameter, Ringsdorf-Werke, Germany) or with a 20-mL thermostated conical cell using a screen-printed electrode (SPE) as the working electrode, an Ag/AgCl (BAS) as reference electrode, and a Pt wire as auxiliary electrode with a gold connecting pin (BAS). All experiments were carried out at room temperature.

A filter spectrophotometer (Metrohm, model 662) was used for performing the reference method based on methylene blue formation in acidic medium.[4] IR and UV−visible spectra were performed by using Perkin-Elmer 577 and P-Elmer Lambda-15 instruments, respectively.

Procedure. The applied potential for the amperometric measurements was +0.08 V versus Ag/AgCl. After the potential had been applied to the SPEs, the background current was allowed to decay to a stable value under mild stirring. Standards or unknown samples were injected, and the increase of the current was recorded by means of an interface card. The steady-state current (within 20 s) was taken as a measure of the analyte concentration.

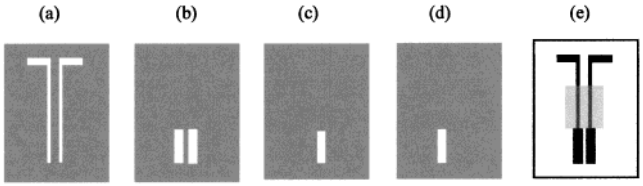

Figure 1. Schematic representation of the screens used for the fabrication of screen printed electrodes: (a) silver layer, (b) overlay pad (graphite layer), (c) Ag/AgCl layer, (d) working layer, and (e) final appearance of the printed sensor (one couple). The shadowed area represents the insulating layer.

The surface coverage Γ of the modifier was evaluated from the integrated anodic peak of the cyclic voltammograms in the range −300 to +50 mV versus Ag/AgCl, at 50 mV s^{-1}, corrected for the background current.

Preparation of the Modified Electrodes. Spectroscopic graphite rods were polished on ultrafine (1200-grit) emery paper (Struers, Salzburg, Austria), then polished against a lens cleaning tissue (No. 105 Whatman), and finally thoroughly washed with double-distilled water. Rods were dried at 60 °C for 30 min, heated in a muffle furnace at 700 °C for 90 s (to remove any small particles from the surface area), and allowed to cool in a desiccator.[15] To avoid electrical contact between the sides of the electrodes and the solution, the sides of the working electrodes were covered with Parafilm before use.

The surface modification was made by applying 10 μL of different concentrations of the $[Sb^{V}O(CHL)_2]$Hex solution in acetone, ranging from 0.3 to 1.5 mM, on the surface of the electrode with a micropipet. The solvent was allowed to evaporate at ambient temperature for 15 min, following thorough washing with distilled water.

Fabrication of Screen-Printed Electrodes. The screens allow ink to pass through a predetermined area that governs the size and the shape of the print, as illustrated in Figure 1. SPEs were printed in arrays of eight couples consisting of a working and a reference electrode. The layers were printed in the following order: first a layer made of silver that acts as the conductive track (Figure 1a), second a carbon layer (overlay pad) ensuring that no contact can be established between the solution and the silver (Figure 1b), and finally, the Ag/AgCl layer over the overlay pad (Figure 1c). Each layer was allowed to dry for 20 min at 60 °C. The working layer (0.2 × 0.4 cm) was printed over the overlay pad (Figure 1d). The printed material was produced by mixing 5 g of graphite powder and 0.5 g of $[Sb^{V}O(CHL)_2]$Hex in 10 mL of 1.5% (w/v) ethyl cellulose in 2-butoxyethyl acetate. Silver rods were covered by applying a nail hardener (which acts as a waterproof insulating layer) leaving their upper part free for electrical connections (Figure 1e, shadowed area).

Sample Preparation. Samples were collected from the sewage treatment plant of the city of Ioannina. Simulated samples (SIM) came from the main stream after spiking known amounts of sodium sulfide. Samples were filtered through a Whatman paper No. 41 in order to remove solid (sludge) waste and were analyzed without further pretreatment. According to the literature, samples were stored at 4 °C under nitrogen atmosphere and analyzed

(15) Polášek, M.; Gorton, L.; Appelqvist, R.; Marko-Varga, G.; Johansson, G.; *Anal. Chim. Acta* **1991**, *246*, 283−292.

Table 1. Elemental Analysis and IR/UV−Visible Data of the $[Sb^{V}O(CHL)_2]$Hex Complex

	elemental analysis (%)							
	theoretical				experimental			
	Sb	C	N	H	Sb	C	N	H
	14.22	46.29	1.64	4.47	13.93	47.11	1.68	5.00
IR spectrum, (cm^{-1})[a]	450−465 m (br), 575−600 vs, 800 vs (br) [ν(Sb═O)], 850 vs [ν(C−Cl)], 1000 vs, 1175 vs and 1215 w [δ(C−H)] in plane, 1305 s, 1340 vs, [ν(C−C)], 1470−1490 s [ν(C−O)], 1565 vs (br) and 1655 vs, [ν(C−O)], 2860−2920 vs [ν(C−H)] aliphatic of hexadecylpiridinium, 3060−3090 m [ν(C−H)] aromatic of hexadecylpiridinium							
UV−visible spectrum[b]	$\log \epsilon_1 = 3.10$ (516.8 nm), $\log \epsilon_2 = 4.58$ (317.6 nm), $\log \epsilon_3 = 4.35$ (258.4 nm).							

[a] The IR spectrum of the complex compound is indicative of three major characteristics: the presence (a) of coordinated chloranilate anions, (b) of hexadecylpyridinium counterions, and (c) of the antimonyl group. The assignment of the bands was based on literature reports. The bands at 1655 and 1565 cm^{-1} are assigned to the C−O stretching vibrations and they are shifted to higher frequencies (1670, 1635, 1555 cm^{-1}) compared with the free ligand, while the same bands in the spectrum of the hexadecylpyridinium salt of the ligand are at 1625 and 1530 cm^{-1}. This can lead us rather safely to the conclusion that chroranilates are strongly bound to the antimonyl group. The broad band at 800 cm^{-1} is attributed to the Sb═O stretching vibrations [b] The molecular absorption coefficients are expressed in M^{-1} cm^{-1}. DMSO was used as solvent throughout. Peaks at 516.8, 317.6, and 258.4 nm are due to n → σ^*, $\pi \rightarrow \pi^*$, and n → σ^* transitions and can be attributed to $^1B_1g \leftarrow {}^1Ag$, $^1B_3u \leftarrow {}^1Ag$, and C═C bonds, respectively.

within two weeks after collection.[16] **Note:** *Sodium sulfide is a corrosive agent and must be handled with extreme caution. Do not inhale vapors!*

Synthesis and characterization of $[Sb^{V}O(CHL)_2]$Hex. Chloranilic acid ($C_6Cl_2O_4H_2$, 2,5-dichloro-2,5-cyclohexadiene-3,6-dioxo-1,4-dione, $pK_1 = 0.58$ and $pK_2 = 2.72$ at 25 °C) and potassium pyroantimonate ($KSb(OH)_6$, $K_2H_2Sb_2O_7$) react in a usual acid−base neutralization reaction, according to the following reactions:[17]

$$KSb(OH)_6 + 2C_6Cl_2O_4H_2 \rightarrow [SbO(C_6Cl_2O_4)_2]K + 5H_2O \quad (2)$$

$$K_2Sb_2H_2O_7 + 4C_6Cl_2O_4H_2 \rightarrow 2[SbO(C_6Cl_2O_4)_2]K + 5H_2O \quad (3)$$

The soluble $[SbO(C_6Cl_2O_4)_2]K$ reacts with hexadecylpyridinium chloride ($C_{21}H_{38}N^+Cl^-$) according to the reaction 4,

$$[SbO(C_6Cl_2O_4)_2]K + C_{21}H_{38}N^+Cl \rightarrow [SbO(C_6Cl_2O_4)_2][C_{21}H_{38}N]\downarrow + KCl \quad (4)$$

leading to the quantitative formation of the final product, $SbNC_{33}H_{38}O_9Cl_4$, in the form of an ion-pair complex compound.

The formation constant of these soluble complex salts seems to be higher than that of the potassiumantimonyl tartrate, $KSbOC_4H_4O_6$, since the addition of ammonia produces no hydrolytic precipitation of basic antimonate salts. The solid reactants in a stoichiometry of 2:1 are thoroughly pulverized in a mortar and then transferred with an excess of distilled water (800 mL) to a beaker. The reaction is taking place in a water bath (70 °C) for 6 h, under stirring. The mother liquid progressively becomes clear with a deep red-violet coloration, presenting a final pH 4−6. The volume of the solution is reduced to 200 mL by evaporation and the reduced volume filtered through a Whatman No. 43 paper and transferred to a hexadecylpyridinium chloride solution. The mixture is left to react for 3 h under stirring and heating on the water bath. The complex is then filtered through a Gooch 3 crucible and washed to almost colorless washings. The compound is dried for three days, under vacuum and over P_4O_{10}. The complex is taken at a 80% yield as microcrystalline carmine red powder. It is insoluble in water and soluble in acetone, ethanol, dimethyl sulfoxide, and dimethylformamide. Elemental analysis and IR/UV−visible data are presented in Table 1. The molecular weight of the product, $SbNC_{33}H_{38}O_9Cl_4$, is 856.22 and its melting point 140 °C.

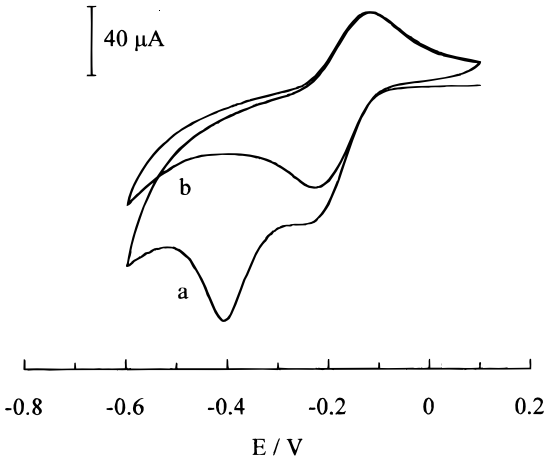

Figure 2. Cyclic voltammograms of a $[Sb^{V}O(CHL)_2]$Hex CME in a 0.25 M phosphate buffer in 1 M KCl, pH 6.5: (a) first scan, (b) next scans. Surface coverage, 1.71 nmol cm^{-2}. Scan rate, 100 mV s^{-1}.

RESULTS AND DISCUSSION

Electrochemistry of the Adsorbed $[Sb^{V}O(CHL)_2]$Hex. The active surface area of the graphite electrodes was previously evaluated applying double-step chronocoulometry and found to be 0.33 ± 0.01 cm^2.[18]

Cyclic voltammetry with $[Sb^{V}O(CHL)_2]$Hex CMEs in 0.25 M phosphate buffer in 1 M KCl, pH 6.5, solution produces well-behaved peaks. The formal potential $E^{o'}$ was calculated by taking the mean of the position of the anodic and cathodic peak potentials and found to be −170 mV versus Ag/AgCl. As it can be seen in Figure 2a, a well-defined peak appears in the cathodic region at −400 mV which is absent in subsequent cycles. This peak is

(16) Lasorsa, B.; Casas, A. *Mar. Chem.* **1996**, *52*, 211−220.
(17) Veltsistas, P. G. Thesis. University of Ioannina, Greece, 1992.
(18) Florou, A. B.; Prodromidis, M. I.; Karayannis, M. I.; Tzouwara-Karayanni, S. M. *Electroanalysis* **1998**, *10*, 1261−1268.

Scheme 1. Irreversible Reduction of Chloranilate

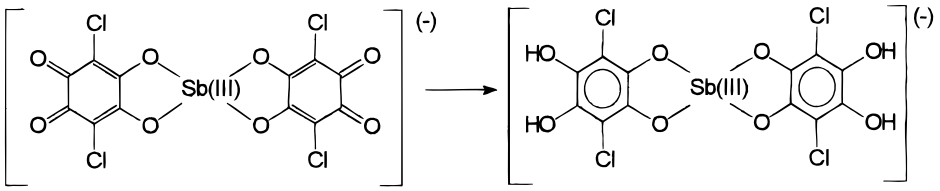

probably due to the irreversible reduction of the ligand (chloranilate) from the quinoidal form to the thermodynamically more stable tetrahydroxy aromatic form (Scheme 1). This multihydroxy moiety highly stabilizes Sb(III) and Sb(V) against hydrolytic procedures.

An important parameter, which should be taken into account during the optimization of a CME, is the surface coverage. Several parameters such as the electron-transfer kinetics between the adsorbed compound and the underlying graphite structure, the stability of the sensor, and the kind of limitations of the produced current (diffusion or kinetic limited) are directly or indirectly affected by its value. The peak current, I_p, for an adsorbed compound is given by the following equation

$$I_p = (n^2F^2/4RT)\Gamma Av \qquad (5)$$

where A is the surface area, Γ the surface coverage, and v the sweep rate.

Figure 3 shows the dependence of the current (the anodic in this case) versus the scan rate (Figure 3A) and the square root of the scan rate (Figure 3B) at four different surface coverages varying from 0.51 to 3.39 nmol cm^{-2}. Plots of Ia versus the scan rate show a linear relation up to 800 mV s^{-1} for low values of Γ (0.51 nmol cm^{-2}). Increasing the value of Γ (1.04 and 1.71 nmol cm^{-2}) reduces linearity to 600 and 500 mV s^{-1}, respectively, and in a regime of high surface coverage (3.39 nmol cm^{-2}) linearity is restricted to 150 mV s^{-1}, indicating a diffusion-limited process rather than a kinetic-limited one, as expected for adsorbed molecules. These conclusions are also strongly supported from plots of Ia versus the square root of the scan rate, where linearity is decreased upon decrease of the surface coverage. For surface coverage higher than 1.71 nmol cm^{-2}, it seems that multilayers begin to form and that the Langmuir model is not followed any more. The experimental data so far (Γ < 1.71 nmol cm^{-2}) supports a model in which the redox compound is adsorbed on the electrode surface. Beyond this value of Γ, the molecules of the modifier are not physically entrapped (or bonded)[19] in the graphite lattice, but they are restrained through weak intermolecular bonds (e.g., van der Waals), thus resulting in a continuous leaking from the multilayer structure. Under these conditions, the diffusional step dominates the procedure, so linearity increases upon increase of the concentration of the modifier (Figure 3B).

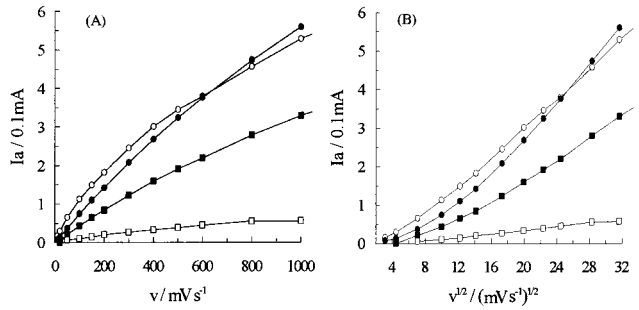

Figure 3. Variation of I_p with (a) the scan rate and (b) the square root of the scan rate at different surface coverages. Surface coverage: (□) 0.51, (■) 1.07, (●) 1.71, and (○) 3.39 nmol cm^{-2}. Buffer, 0.25 M phosphate in 1 M KCl, pH 6.5.

Table 2. Electrochemical Characteristics and Kinetic Data of Immobilized [Sb^{V}O(CHL)$_2$]Hex

Γ (nmol cm^{-2})	ΔE_p[a] (mV)	Ia/Ic[a]	k^o (s^{-1})	α_a	α_c
0.51	33	0.96	33 ± 4	0.51	0.55
1.04	41	0.96	16 ± 2	0.53	0.60
1.71	47	1.06	12 ± 2	0.46	0.47
3.39	58	1.10	9 ± 1	0.7	0.8

[a] Scan rate, 50 mV s^{-1}.

Table 3. Slope Modification of the Ia = $f(\Gamma)$ Plots at Different Scan Rates: Γ_1 = 0.51 nmol cm^{-2}, Γ_2 = 1.04 nmol cm^{-2}, Γ_3 = 1.71 nmol cm^{-2}, and Γ_4 = 3.39 nmol cm^{-2}

	scan rate (mV s^{-1})			
dIa/dΓ	100	200	300	400
dIa/d$\Gamma_{1/2} = D_1$	6.7	13.1	19.6	25.4
D_2/D_1	*0.71*	*0.71*	*0.67*	*0.67*
dIa/d$\Gamma_{2/3} = D_2$	4.9	9.1	13.2	16.9
D_3/D_2	*0.39*	*0.22*	*0.14*	*0.10*
dIa/d$\Gamma_{3/4} = D_3$	1.9	2.0	1.9	1.7

The extended linearity upon increase of the scan rate is also a criterion for the fast kinetics of the adsorbed species. The sharp restriction of the linearity when surface coverage increases from 1.71 to 3.39 nmol cm^{-2} could also be attributed to the delocalization of antimony in the multilayer structure. More evidence supporting this conclusion comes from the values of ΔE_p (Table 2) and the slope modification (dIa/dΓ) (Table 3) observed for surface coverage higher than 1.71 nmol cm^{-2}. This is a critical value of surface coverage over which the interactions between the redox species result in peak broadening, indicative of the formation of multilayers.[18]

According to eq 5, the current is proportional to the surface coverage. Dividing the total surface of the electrode into the diameter of the redox molecule, it is possible to calculate (theoretically) the number of redox species that obey eq 5 (monolayer formation, Langmuir model), assuming that the molecule is spherical and the electrode surface is homogeneous without cavities, reaching thus its macroscopic geometrical value πR^2. When the population of redox molecules exceeds this number

(19) Gorton, L. *Electroanalysis* **1995**, *7*, 23−45.

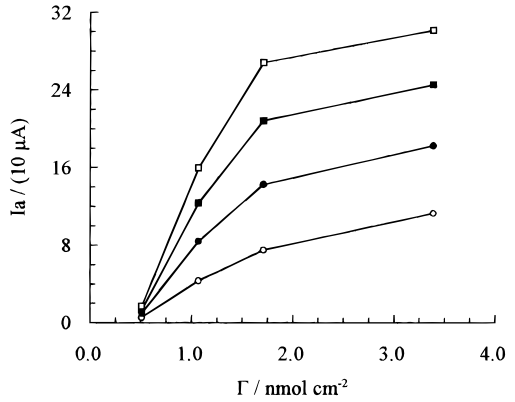

Figure 4. Dependence of Ia on surface coverages at different scan rates. Scan rates: (○) 100, (●) 200, (■) 300, and (□) 400 mV s^{-1}. Buffer, 0.25 M phosphate in 1 M KCl, pH 6.5.

Scheme 2. Catalytic Regenerated EC Mechanism, Where k^o Is the Electrochemical Rate Constant of the $[Sb^VO(CHL)_2]Hex$ Redox Couple Immobilized on the Graphite Surface

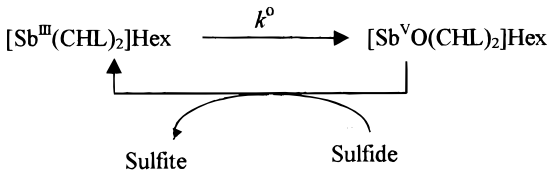

(surface saturation), the current increase is not proportional to the redox population, as steric and overlapping effects result in a decrease of the rate of increase of the current to the surface coverage (Figure 4). This phenomenon is clearer at high scan rates as the molecules beyond the saturation coverage follow partly a diffusional model where the current is proportional to the square root of the rate, in contrast to the adsorbed species where the current is directly proportional to the scan rate. In Table 3, we have calculated the quantity $dIa/d\Gamma$ for the tested surface coverages at 100, 200, 300, and 400 mV s^{-1}. The fact that D_2 is always lower than D_1 is indicative of the saturation of the surface electrode rather than of formation of multilayers. The ratio D_2/D_1 is almost the same at all the tested scan rates and, as expected, even within the statistical error of this calculation, is lower at high scan rates. At higher surface coverage, D_3 is much lower, taking values almost half of these of D_2 for low scan rates (4.9−1.9) and one-tenth (16.9−1.7) for higher scan rates. Slope modification is obvious if we calculate the ratio D_3/D_2. As expected the received values are much lower than D_2/D_1. This phenomenon becomes more obvious as the scan rate increases.

Deviations from the ideal values of ΔE_p seem to be usual for redox-modified electrodes, even at low coverages and sweep rates because of the interactions between the $[Sb^VO(CHL)_2]Hex$ molecules or their interaction with the support. Broader and flatter peaks can be also attributed to the influence of heterogeneity of the electrode.[20]

The number of the participating electrons in the redox reaction can be evaluated from the slope of the linear part of the curve for $\Gamma = 1.71$ nmol cm^{-2}, in Figure 3A (eq 5) as 1.46 ± 0.03. This result suggests two successive single electron-transfer steps rather than two electron-transfer reactions in one step.

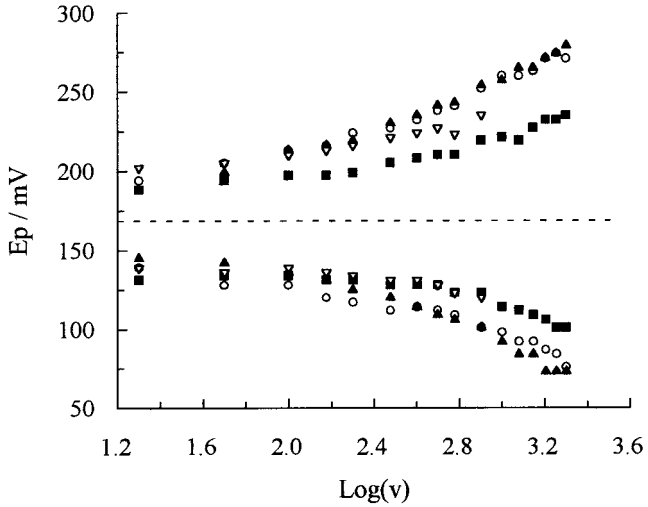

Figure 5. Dependence of E_p on log(v) at different surface coverages. Surface coverage: (■) 0.51, (○) 1.71, (▽) 1.07, and (▲) 3.39 nmol cm^{-2}. Buffer, 0.25 M phosphate in 1 M KCl, pH 6.5.

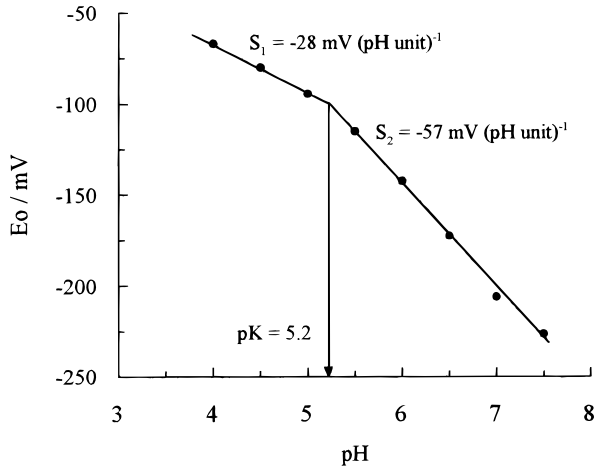

Figure 6. Formal potentials $E^{o'}$ for adsorbed $[Sb^VO(CHL)_2]Hex$ as a function of pH: scan rate, 50 mV s^{-1}. Buffer, 0.25 M phosphate in 1 M KCl. Surface coverage, 1.71 nmol cm^{-2}.

The apparent electrochemical (self-exchange) rate constant k^o (Scheme 2) was calculated from Tafel diagrams according to the method described by Laviron.[21] Anodic, α_a, and cathodic, α_c, transfer coefficients and k^o were calculated from the slopes and intercepts of plots E_p versus log(v), for high scan rates at different surface coverages. Figure 5 illustrates the plots used for evaluating α_a and k^o from the anodic as well as α_c and k^o from the cathodic partial reaction. The slope of the linear segment is equal to $-2.303RT/\alpha_c nF$ for the cathodic and $2.303RT/\alpha_a nF$ for the anodic peak. The evaluated values for the coefficients α_a and α_c and the k^o are illustrated in Table 2. The sum of transfer coefficients α_c and α_a is close to its normal value of 1, expect in the case of high surface coverage.

A value of k^o varying from 9 to 33 s^{-1} (Table 2) was evaluated from all the extracted experimental data applying equation $k^o = 2.303\alpha_c nFv_o/RT$, using a value of $a = 0.5$.[21] Apart from the fast electron kinetics and screening of redox metal (see above), the large value of k^o also justifies fast establishment of the equilibrium.

(20) Laviron, E.; Roullier, L. *J. Electroanal. Chem.* **1980**, *115*, 65−74.

(21) Laviron, E. *J. Electroanal. Chem.* **1979**, *101*, 19−28.

Scheme 3. Reduction of the Mediator through a $2H^+$ Mechanism

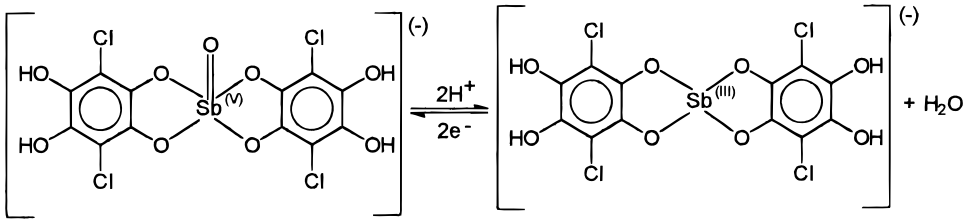

The dependence of the formal redox potential $E^{o'}$, for adsorbed $[Sb^{V}O(CHL)_2]$Hex, on the pH was investigated by cyclic voltammetry. Figure 6 shows $E^{o'}$ as a function of pH. The $E^{o'}$ value was taken at scan rate 50 mV s^{-1}, where no kinetic effects would adversely distort the peak current.[21]

A pK_a value of 5.2 ± 0.2 for the $[Sb^{III}(CHL)_2]$Hex was found from the intersection of the two straight lines with slopes −28 mV (pH unit)$^{-1}$ in the acid region and −57 mV (pH unit)$^{-1}$ in the more alkaline region. The change in the slope from −28 to −57 mV (pH unit)$^{-1}$ is caused by the oxidized form of $[Sb^{V}O(CHL)_2]$-Hex.[21] According to the calculated slopes, the reduction of the mediator could be performed either through a $2H^+$ (pH >5.2) or a $1H^+$ mechanism (pH <5.2). The reduction of $[Sb^{V}O(CHL)_2]$Hex, through a $2H^+$ mechanism, is illustrated in Scheme 3. The reduction of $[Sb^{V}O(CHL)_2]$Hex, through a $1H^+$ mechanism, probably produces a complex where antimony is at the oxidation state four. The only rational way for this procedure to be explained is the acceptance of a charge-transfer, mixed-valence (Sb^{III}/Sb^{V}) system.[22,23]

Electrocatalytic Oxidation of Sulfide. The coupling efficiency between the immobilized mediator $[Sb^{V}O(CHL)_2]$Hex and sulfide was studied with cyclic voltammetry (Figure 7A). The $[Sb^{V}O$-$(CHL)_2]$Hex-modified electrodes in the working buffer gave rise to a reversible pair of redox waves with a cathodic peak potential E_{pc} of −212 mV and an anodic peak potential E_{pa} of −132 mV versus Ag/AgCl (Figure 7A, scan a). Scan c is a voltammogram of sodium sulfide solution taken with a plain graphite electrode for comparison. The sulfide oxidation on the plain electrode (scan c) appears at +400 to +500 mV in agreement with earlier reports.[13] Oxidation of sulfide on the $[Sb^{V}O(CHL)_2]$Hex-modified electrodes gives a peak at −100 mV (scan b), very close to the formal potential of the adsorbed mediator (scan a). Addition of sodium sulfide to the working solution and subsequent scanning over the same potential range (Figure 7A, scan b) results in a large increase in current in the anodic region due to the fact that the sulfide present in the solution reduces the oxidized form of the immobilized mediator, $[Sb^{V}O(CHL)_2]$Hex. As $[Sb^{III}(CHL)_2]$Hex is regenerated from the reaction of $[Sb^{V}O(CHL)_2]$Hex with sulfide during the sweep, there is a significant increase in the anodic current and a corresponding decrease in the accompanying reduction in the cathodic region. These results are indicative of fast electrocatalysis which occurs at or near a diffusion-controlled rate.[24]

Despite their efficiency in promoting the electrocatalysis of sulfide, $[Sb^{V}O(CHL)_2]$Hex-modified electrodes were not used further in analytical applications, as their stability did not meet the standards of CMEs. After 300 successive scans, a continuous leaking of the modifier from the electrode surface was observed, leading to a progressive reduction of the anodic current. At surface coverage of 2.5 nmol cm^{-2}, at pH 6.5, the sensor retains only the 60−65% of its initial activity. This phenomenon is due to the formation of multilayers and the weak nature of the bonds, which constrain the layers. Lower concentrations of the modifier showed a better stability (up to 75% of the initial activity); however, the electrodes were not suitable for analytical applications.

To overcome this problem, screen-printed electrodes were fabricated. SPEs maintained the good characteristics of CMEs in terms of coupling efficiency (electrocatalysis) of sulfide. Moreover, they showed good working and storage stability. Polymer con-

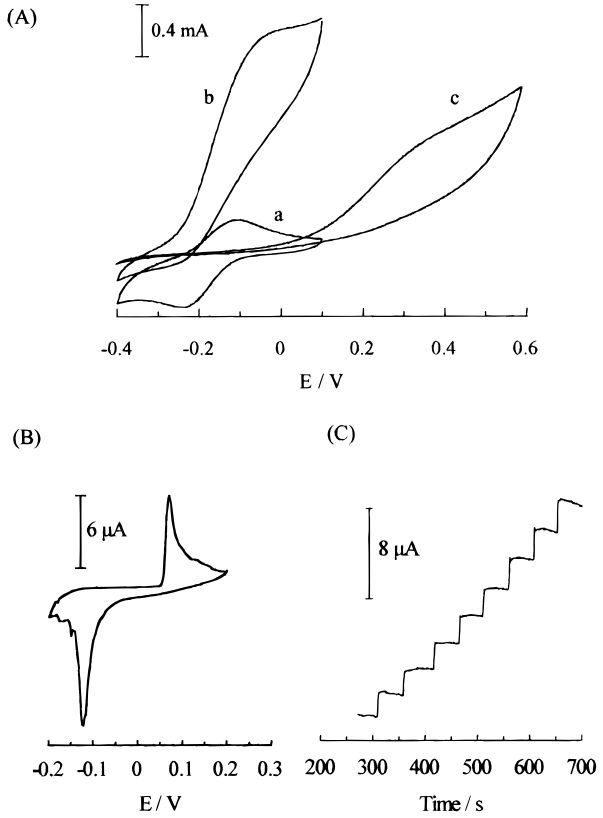

Figure 7. (A) Cyclic voltammograms illustrating the catalytic oxidation of sulfide mediated by adsorbed $[Sb^{V}O(CHL)_2]$Hex: (a) $[Sb^{V}O(CHL)_2]$Hex CME in buffer solution (Γ = 2.5 nmol cm^{-2}); (b) the same $[Sb^{V}O(CHL)_2]$Hex CME in a buffer solution containing 3 mM sulfide; (c) graphite electrode (plain) in a buffer solution containing 3 mM sodium sulfide. (B) Cyclic voltammogram of $[Sb^{V}O(CHL)_2]$Hex printed electrode. Scan rate, 50 mV s^{-1}. Buffer, 0.25 M phosphate in 1 M KCl, pH 6.5. (C) Repeatability of the results for 0.1 mM sodium sulfide using $[Sb^{V}O(CHL)_2]$Hex-printed electrode.

(22) Allen, G. C.; Hush, N. S. In *Progress in Inorganic Chemistry*; Cotton, F. A., Ed.; Interscience Publishers: New York, 1967; Vol. 8, pp 357−390.
(23) Bailar, J. C. *Comprehensive Inorganic Chemistry*; Pergamon Press: New York, 1975; Vol.2
(24) Rocklin, R. D.; Murray, R. C. *J. Phys. Chem.* **1981**, *85*, 2104−2112.

centrations of 1, 1.5, and 2% (w/v) were investigated, by fabricating three different batches of SPEs containing the corresponding concentration of ethyl cellulose. Permselective properties of the tested polymer concentrations were studied with amperometry, using sulfide (mol wt 32) and ascorbic acid (mol wt 172) as model compounds. A concentration of 1.5% (w/v) was finally selected, as it ensures very good stability (retention of the modifier), good selectivity (based on size exclusion properties of the membrane), and satisfactory sensitivity for sulfide (data not shown).

SPE was merely the improvement of the working stability of the $[Sb^{V}O(CHL)_2]$Hex CMEs due to the retention properties of the ethyl cellulosic film. Furthermore, this type of sensor is very inexpensive and easy to produce in great numbers, thus making it ideal for single use. The latter feature is of great interest for environmental applications, especially in the case of toxic samples.

The quality of printed sensors is checked by applying cyclic voltammetry. As shown in Figure 7B, the anodic peak, which is responsible for the electrocatalysis of sulfide, appears at +80 mV versus the printed Ag/AgCl reference electrode. The shift of the oxidation potential is not due to the different nature of the reference electrode but to the different nature of the immobilized mediator. The same cyclic voltammogram was recorded when the commercial reference electrode (BAS) was used. The nature of the immobilized mediator (high concentration, entrapment in the polymeric film) is also responsible for the larger peak potential separation.

The reproducibility of fabrication was checked by applying amperometry on a 0.1 mM solution of sodium sulfide with 10 randomly chosen electrodes and found to be 4.2%. This deviation is satisfactory and can be further improved using screens of higher mesh, as this parameter is responsible for the texture and the size of the printed (working) area. The reproducibility of fabrication is also a matter of printer quality; however, the used printer offers high reproducibility of the applied pressure and speed of the squeegee.

The dependence of the electrocatalysis of sulfide on the pH was investigated within the pH range 5.0−7.5 (data not shown). More acidic conditions result in increased volatility of the analyte, while for values higher than pH 7.5, the electrochemical behavior of the mediator is not clear (peak broadening, low current intensities). The value of 6.5 was finally selected, taking into account the relatively low volatility of the analyte and the optimum efficiency of the sensor at this pH value.

Good linearity, 0.01−0.7 mM sulfide, for the $[Sb^{V}O(CHL)_2]$Hex-printed electrodes ($r = 0.999$), was achieved. The detection limit (signal/noise ratio 3) was 5 μM. The relative standard deviation (RSD) for a standard solution of 0.1 mM sodium sulfide was 2.8% ($n = 8$).

The proposed method was applied to wastewater-simulated samples for the determination of sulfide. The results of various samples are summarized in Table 4. The results were compared with those obtained with a spectrophotometric reference method.[4] The mean relative error was 2.4%. The accuracy of the method was also verified by recovery studies adding standard sodium sulfide solutions to samples. Recoveries of 94−102% were achieved, as shown in Table 5.

Interferences. $[Sb^{V}O(CHL)_2]$Hex CMEs and screen-printed electrodes bearing $[Sb^{V}O(CHL)_2]$Hex showed a remarkable selectivity toward sulfide. Their response in the presence of a big variety of reducing compounds was almost not detectable. The selectivity of antimony toward sulfide is well known, and antimony(V) chloride was used for the qualitative determination of sulfide.[25] This selectivity is further enhanced in this study as the selected concentration of the ethyl cellulose membrane in SPE offers permselectivity based on size exclusion. Interference from various reductive species was investigated by applying the method of mixed solutions in the presence of 0.1 mM sodium sulfide. Some of these do not exist in trivial wastewater samples; however, they are tested in order to check the selectivity of the proposed sensor against the most popular reductive species. The relative responses for 2 mM ampicilin, 4 mM theophyline, 4 mM glutathione, 2 mM uric acid, 2 mM cysteine, 2 mM homocysteine, 4 mM paracetamol, 3 mM ascorbic acid, 2 mM thiamine, 2 mM riboflavin, 5 mM NADH, 1 mM penicillamine, 5 mM sulfite, 5 mM sodium dithionite, 2 mM parathion, 2 mM malathion, and 2 mM solutions of pesticides Methomyl and Lannate were 102, 103, 104, 102, 104, 103, 103, 105, 108, 105, 104, 100, 103, 104, 104, 102, 102, and 102%, respectively, compared to the response shown with pure solution of 0.1 mM sulfide taken as 100%.

In the case of metal cations, 2 mM solutions of the corresponding nitrate or chloride salts were analyzed without sulfide present because it is known that metal ions form insoluble sulfides. The response for Sn^{2+}, Co^{2+}, Pb^{2+}, Zn^{2+}, Cu^{2+}, Ni^{2+}, Mn^{2+}, Mg^{2+}, Fe^{3+}, and Fe^{2+} was not detectable. Anions (SCN^-, CN^-, I^-, NO_2^-, and CO_3^{2-}) were also tested at a concentration of 2 mM and no interference effect was observed.

Stability of the Sensor. The working stability of the adsorbed $[Sb^{V}O(CHL)_2]$Hex was verified by monitoring the remaining amount of the active substance after 300 successive sweeps. The amount of $[Sb^{V}O(CHL)_2]$Hex remaining on the electrode surface is almost 70% of the original value for surface coverage between 2.0 and 2.5 nmol cm^{-2}. However, the storage stability of the chemically modified electrodes was very good as the electrodes were found to have reserved their initial activity for more than two months when kept at 4 °C.

Table 4. Determination of Sulfide in Wastewater Samples

sample	proposed method[a] ($\times 10^{-4}$ M)	reference method ($\times 10^{-4}$ M)	rel error (%)
Sim.1	1.10 ± 0.08	1.13	−2.8
Sim.2	1.50 ± 0.06	1.52	−1.3
Sim.3	2.00 ± 0.09	1.96	+2.0
Sim.4	2.50 ± 0.1	2.43	+2.8

[a] Average of three runs ± SD.

Table 5. Recovery of Sulfide Added to Real Samples

sample	added (mM)	found (mM)	recovery (%)
Sim.1	0.100	0.092	92
Sim.2	0.100	0.097	97
Sim.3	0.100	0.098	98
Sim.4	0.100	0.102	102

(25) Feigl, F.; Anger, V. *Spot Tests in Inorganic Analysis*, 6th ed.; Elsevier: Amsterdam, 1972.;

Screen-printed electrodes explore a prolonged working and storage stability. The working stability of the sensors was studied by continuous exposure to the working buffer, measuring the produced current after the injection of a 0.2 mM solution of sodium sulfide. As a result, the final activity (current response versus initial current response × 100%) was 95% after 100−120 injections. The same electrode could be used for at least three days (storage at room temperature, continuous use). A mean loss of its initial activity of ∼10% was observed daily. Printed sensors also displayed good storage stability if stored dry at 4 °C when not in use. They retained their initial activity for more than four months.

ACKNOWLEDGMENT

The authors thank Dr. G. Pilidis for valuable discussion concerning the equilibrium schemes of the $[Sb^{V}O(CHL)_2]$Hex molecule. Thanks are also extended to Ph.D. candidate Mrs. A. Florou for her important assistance during the completion of this work.

Received for review February 11, 2000. Accepted June 14, 2000.

AC0001784